

Photooxidative removal of Hg⁰ from simulated flue gas using UV/H₂O₂ advanced oxidation process: Influence of operational parameters

Bo Zhang, Zhaoping Zhong[†], Kuan Ding, and Lulu Yu

Key Laboratory of Energy Thermal Conversion and Control of Ministry of Education,
School of Energy and Environment, Southeast University, Nanjing 210096, China
(Received 26 March 2013 • accepted 16 September 2013)

Abstract—Element mercury (Hg⁰) from flue gas is difficult to remove because of its low solubility in water and high volatility. A new technology for photooxidative removal of Hg⁰ with an ultraviolet (UV)/H₂O₂ advanced oxidation process is studied in an efficient laboratory-scale bubble column reactor. Influence of several key operational parameters on Hg⁰ removal efficiency is investigated. The results show that an increase in the UV light power, H₂O₂ initial concentration or H₂O₂ solution volume will enhance Hg⁰ removal. The Hg⁰ removal is inhibited by an increase of the Hg⁰ initial concentration. The solution initial pH and pH conditioning agent have a remarkable synergistic effect. The highest Hg⁰ removal efficiencies are achieved at the UV light power of 36 W, H₂O₂ initial concentration of 0.125 mol/L, Hg⁰ initial concentration of 25.3 μg/Nm³, solution initial pH of 5, H₂O₂ solution volume of 600 ml, respectively. In addition, the O₂ percentage has little effect on the Hg⁰ removal efficiency. This study is beneficial for the potential practical application of Hg⁰ removal from coal-fired flue gas with UV/H₂O₂ advanced oxidation process.

Keywords: Photooxidative Removal, Hg⁰, UV/H₂O₂ Advanced Oxidation Process, Operational Parameters

INTRODUCTION

Mercury (Hg) is a potent neurotoxin which can cause bio-accumulation as methylmercury, and it is commonly regarded as one of the extremely toxic heavy metals [1-3]. The residence time of mercury in the atmosphere can be as long as approximately two years according to reports [4]. Clearly, mercury pollution in air is causing increasing concern.

Coal-fired utilities are the main anthropogenic source of mercury emissions and have already become the global focus [5-7]. Mercury content in coal is 0.02-1.0 μg/g, and the mercury concentration in flue gas from coal combustion is at microgram-per-cubic-meter level, in quantities ranging from a few micrograms per cubic meter to several tens of micrograms per cubic meter. Mercury discharged into the atmosphere through coal combustion exists in three species: element mercury (Hg⁰), oxidized mercury (Hg²⁺) and particulate mercury (Hg^p) [3,8]. As reported, Hg²⁺ and Hg^p can be removed by current air pollution control devices, such as electrostatic precipitator, bag house filter and wet flue gas desulfurization [3,9]. However, Hg⁰ is hardly captured by these devices because of its low solubility in water and high volatility [10]. Prestbo et al. [11] studied the mercury emission of fourteen coal-fired power plants. They found that Hg⁰ can account for up to 60% of the total mercury in some cases. Zhang et al. [12] reported a higher proportion of Hg⁰ (>90%) in flue gas. Obviously, Hg⁰ is the main Hg species emitted to the atmosphere. As a result, Hg⁰ can cause global mercury pollution easily through the motions of the atmosphere. Therefore, the dis-

covery of Hg⁰ removal technologies is a great challenge.

Adsorption technology is effective in removing mercury, which has been a subject of great attention. However, several obvious drawbacks restrict its wide application, such as high cost, competition adsorption, narrow adsorption temperature range and poor regeneration performance [13]. Promoting Hg⁰ oxidation is another useful technology for the removal of Hg⁰, on the basis that Hg²⁺ can be removed through the pollution control devices. Hence, the UV/H₂O₂ advanced oxidation process, employing UV light radiation with hydrogen peroxide oxidation, is a good choice to control Hg⁰. UV/H₂O₂ advanced oxidation is based on the photolysis of hydrogen peroxide and the generation of •OH free radicals [14,15]. •OH free radical is a strong oxidant with a high oxidation potential of 2.8 eV, which can non-selectively react with a wide variety of contaminants at a high reaction rate (10⁸-10¹⁰ L/(mol·s)) [16].

As a new and effective technology, the UV/H₂O₂ advanced oxidation process has significant advantages of mild reaction conditions, simple equipment, lower energy consumption and fewer secondary pollutants [16-20]. Actually, this process has been successfully applied to decompose pollutants from water and air. In the water treatment field, Modirshahla et al. [21] used the UV/H₂O₂ process for the photooxidative degradation of malachite green (MG) and investigated the influence of operational parameters. Yuan et al. [22] investigated the photodegradation of antibiotics in UV/H₂O₂ process and obtained satisfactory results. In the gas purification field, Alibegic et al. [23] studied the kinetics of tetrachloroethylene (PCE) degradation and byproducts formation in the UV/H₂O₂ treatment process. Other researchers [24-26] applied this process to oxidize nitric oxides (NO) in simulated flue gas. However, the UV/H₂O₂ process has not been used for the control of Hg⁰ from flue gas.

We studied the photooxidative removal of Hg⁰ from simulated flue gas using UV/H₂O₂ advanced oxidation process for the first

[†]To whom correspondence should be addressed.

E-mail: zhangbo8848@yeah.net, zhangboforever@163.com,
zzhong@seu.edu.cn

Copyright by The Korean Institute of Chemical Engineers.

time in the world. A laboratory-scale bubble column reactor was designed for simulated flue gas scrubbing. The current study focuses on some key operational parameters influencing the removal efficiency of Hg⁰ (UV light power, H₂O₂ initial concentration, Hg⁰ initial concentration, solution initial pH, pH conditioning agent, O₂ percentage and H₂O₂ solution volume). It is obviously beneficial for the determination of optimal conditions and the practical application of Hg⁰ control from coal-fired flue gas by UV/H₂O₂ advanced oxidation process.

EXPERIMENTAL SECTION

1. Experimental Apparatus

The schematic experimental setup, shown in Fig. 1, consists of the gas supply, laboratory-scale bubble column reactor and analytical detection system. The bubble column reactor [13] (inner diameter: 50 mm; height: 500 mm), made of polymethyl methacrylate, is the most important part. The top of the reactor is covered with a rubber plug [18]. A UV light [19] (Nanjing Huaqiang Electronics Co. Ltd.; diameter: 20 mm; length: 330 mm; dominant wavelength: 254.7 nm) is set inside a quartz casing [20] (outside diameter: 35 mm). Both the UV light and the quartz casing are fixed to the rubber plug and set into the reactor. A gas distributor device [15] (diameter: 50 mm; height: 8 mm; average pore size: 20 μm), made of stainless steel, is used to obtain a uniform distribution of the simulated flue gas from gas inlet chamber [14]. H₂O₂ solution is added into

or moved out of the reactor by opening the rubber plug. Temperature-controlled water bath [6], circulating pump [21] and jacket heat exchanger [16] are used to keep the reaction temperature suitable and constant during the experiment.

Mercury permeation cell [3] (Suzhou Qing'an Instrument Co. Ltd.) is the mercury source, and can produce trace amount of element mercury vapor (Hg⁰) into carrier gas stream per unit time at a given water bath temperature. The mercury permeation cell is secured in a sealed U-tube [4] immersed in a temperature-controlled water bath [5]. Inside the inlet pipe of the U-tube, there are some small glass beads used for the dispersal of gas flow and the equilibrium of temperature. A constant volume of nitrogen flow, from N₂ gas cylinder [2], is fed through the U-tube and acts as the Hg⁰ laden carrier gas stream. The concentration of Hg⁰ in the simulated flue gas can be adjusted by varying the water bath [5] temperature and the simulated flue gas flow rate.

N₂ gas, O₂ gas and (N₂+Hg⁰) gas are mixed in a gas mixer [10] to obtain the desired concentration. The simulated flue gas flow path is determined by switching valves [11,12]. The Hg⁰ initial concentration is measured through the gas bypass (A). The simulated flue gas is passed through the bubble column reactor for Hg⁰ removal through the primary gas path (B). The concentration of Hg⁰ is measured by a mercury analyzer [23] (VM3000 Mercury Vapor Monitor, Mercury Instruments, Germany) continuously, based on cold vapor absorption spectrometry. The measuring range of the mercury analyzer is 0-100 μg/Nm³, and the measuring accuracy is 0.1 μg/Nm³, so accurate measurement of Hg⁰ concentration can be ensured.

Finally, an adsorbing container [24] of activated carbon fiber is used to adsorb the remaining Hg⁰, avoiding environmental pollution. In addition, a gas condenser [22] is designed to remove water vapor from effluent gas, as too much water vapor is harmful to the mercury analyzer. Meanwhile, the pipes, which element mercury vapor traverses, are wrapped by heater bands to prevent the adsorption or condensation of Hg⁰ on pipe walls.

2. Experimental Procedure

Prior to the beginning of the experiments, the experimental setup is operated over a 7-9 days period without H₂O₂ solution or UV light illumination to stabilize the mercury permeation cell and other components, so that the experimental setup itself does not cause a change of Hg⁰ concentration during the experiments.

During the experiments, a series of measures are taken. First, a regulated volume of H₂O₂ solution is prepared with a 30% H₂O₂ solution (Shanghai Chemical Reagent Co., AR) and deionized water according to the required concentration. Then, the initial pH value of the solution is adjusted through the addition of either hydrochloric acid (HCl, 0.5 mol/L) or sodium hydroxide (NaOH, 0.5 mol/L) solution with the use of an acidimeter (PHB-3, Shanghai Leici Instrument Co.). The prepared solution is added into the bubble column reactor.

Second, N₂ gas, O₂ gas and Hg⁰ vapor, from the cylinders (Nanjing Specialty Gas Production Plants, high-purity gases) and the mercury permeation device, are chosen to simulate the flue gas. The total gas flow rate and O₂ concentration are adjusted by regulating the flowmeters [7,8]. Meanwhile, the flow rate of Hg⁰ laden carrier gas stream is kept constant, 200 ml/min, by regulating the flowmeters [9]. Then, the simulated flue gas is forced into the gas mixer for a good mixing result. The initial concentration of Hg⁰ is measured

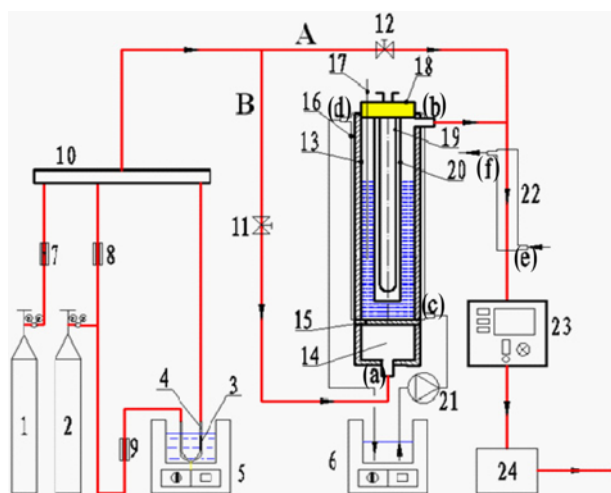


Fig. 1. Schematic diagram of the experimental setup.

- | | |
|---|---------------------------|
| 1. O ₂ gas cylinder | 15. Gas distributor |
| 2. N ₂ gas cylinder | 16. Jacket heat exchanger |
| 3. Mercury permeation cell | 17. Mercury thermometer |
| 4. U-tube | 18. Rubber plug |
| 5-6. Temperature-controlled water baths | 19. UV light |
| 7-9. Flowmeters | 20. Quartz casing |
| 10. Gas mixer | 21. Circulating pump |
| 11-12. Valves | 22. Gas condenser |
| 13. Bubble column reactor | 23. Mercury analyzer |
| 14. Gas inlet chamber | 24. Adsorbing container |
| (a) Gas inlet | (d) Thermal water outlet |
| (b) Gas outlet | (e) Cooling water inlet |
| (c) Thermal water inlet | (f) Cooling water outlet |

Table 1. Constant conditions for removal process

Simulated flue gas compositions	Solution	Reaction temperature/K	Hg ⁰ laden carrier gas flow rate/(ml·min ⁻¹)	Total gas flow rate/(L·min ⁻¹)
N ₂ , O ₂ , Hg ⁰	H ₂ O ₂ solution	298	200	2

by the mercury analyzer when its value becomes stable, through the gas bypass (A) by opening the valve [12] and closing the valve [11].

Third, the simulated flue gas is fed into the bubble column reactor through the primary gas path (B) by closing the valve [12] and opening the valve [11]. The reaction temperature is kept constant at 298 K by adjusting the temperature of the water bath [6], and is monitored by a mercury thermometer [17]. Then, the UV light is turned on when the system is steady. Throughout the experiment, Hg⁰ from the simulated flue gas is scrubbed and removed in the bubble column reactor and the outlet concentration of Hg⁰ is measured simultaneously by the mercury analyzer. The running time of each experiment is 30 minutes, and one datum is recorded every 2 minutes. The remaining pollutants from the simulated flue gas are further removed by the adsorbing container.

3. Data Processing

Each experiment runs 30 minutes and one datum (outlet concentration of Hg⁰) is achieved every 2 minutes. The average of the experimental data within 30 minutes is used as the outlet concentration, and the target pollutant removal efficiency η is calculated according to Eq. (1):

$$\eta = \frac{C_{in} - C_{out}}{C_{in}} \times 100\% \quad (1)$$

where η is the removal efficiency of Hg⁰, C_{in} is the inlet concentration of Hg⁰ and C_{out} is the outlet concentration of Hg⁰.

RESULTS AND DISCUSSION

The constant conditions throughout the experiment are summarized in Table 1.

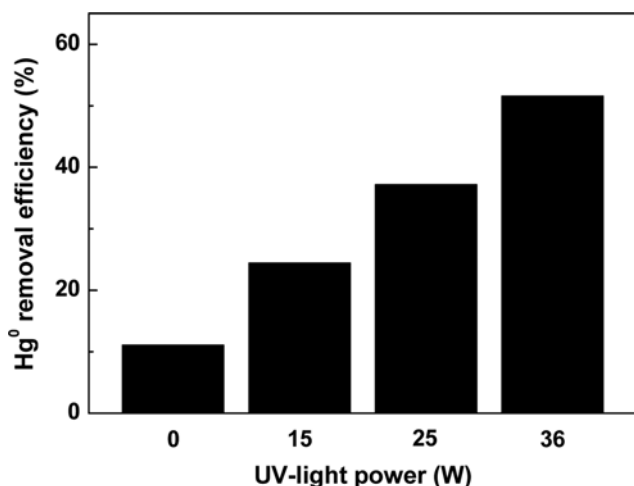


Fig. 2. Removal efficiencies of Hg⁰ under different UV-light powers. Conditions: H₂O₂ initial concentration, 0.075 mol/L; Hg⁰ initial concentration, 77.7–84.8 μg/Nm³; solution initial pH, 7; O₂ percentage, 6%; H₂O₂ solution volume, 600 ml.

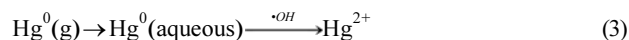
1. Influence of UV Light Power

UV lights with different powers (15, 25 and 36 W, respectively) are used in this experiment, and the influence of UV light power on Hg⁰ removal efficiency is shown in Fig. 2. It is found that 11.1% of Hg⁰ is removed when the UV light power is 0, indicating that the H₂O₂ system without UV radiation also has removal ability for Hg⁰, and Hg⁰ is mainly removed by the oxidation of H₂O₂ on this condition. When the UV light power increases from 0 to 15 W, the Hg⁰ removal efficiency has an apparent increase, which suggests that the UV radiation plays an important role. Moreover, Hg⁰ removal efficiency increases steadily from 24.4 to 51.6% with the increasing of UV light power from 15 to 36 W.

The cooperative mechanism between the H₂O₂ and UV can be explained by the following reaction [27]:



H₂O₂ can absorb above its UV cutoff of 212 nm and below the maximum of 300 nm [20]. As a result, the high energy of UV light causes the photolysis of H₂O₂ and the generation of $\cdot\text{OH}$ free radicals. $\cdot\text{OH}$ free radicals, which has a high oxidation potential ($E^0=2.8$ eV), can remove Hg⁰ by oxidation reaction as Eq. (3). Furthermore, according to Eq. (2), the concentration of generated $\cdot\text{OH}$ free radicals depends directly on the UV incident power when H₂O₂ concentration is fixed. Hence, the increase in the UV light power will improve the yield of $\cdot\text{OH}$ free radicals and, finally, increase the Hg⁰ removal efficiency.



2. Influence of H₂O₂ Initial Concentration

Experiments with different H₂O₂ initial concentrations were also performed, and the results are shown in Fig. 3. Obviously, the H₂O₂ initial concentration has a great impact on Hg⁰ removal efficiency.

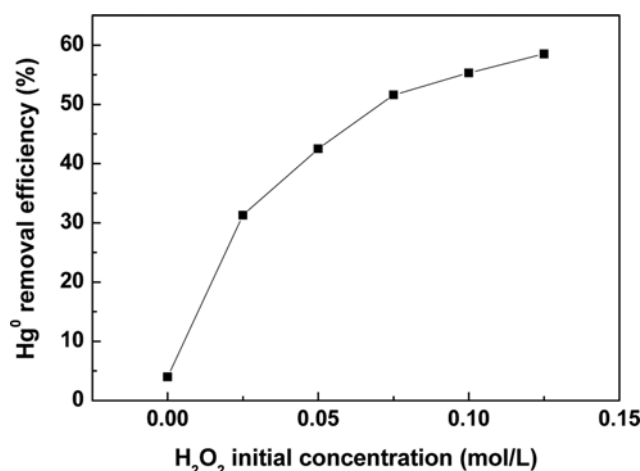


Fig. 3. Removal efficiencies of Hg⁰ under different H₂O₂ initial concentrations. Conditions: UV light power, 36 W; Hg⁰ initial concentration, 77.4–83.5 μg/Nm³; solution initial pH, 7; O₂ percentage, 6%; H₂O₂ solution volume, 600 ml.

In the absence of H₂O₂ the Hg⁰ removal efficiency is nearly negligible, suggesting that a sole UV system has almost no ability to remove Hg⁰. When the H₂O₂ initial concentration increases from 0 to 0.075 mol/L, the Hg⁰ removal efficiency increases greatly from 4.0 to 51.6%. However, with a further increase in the H₂O₂ initial concentration from 0.075 to 0.125 mol/L, the Hg⁰ removal efficiency only has a slight increase. H₂O₂ initial concentration of 0.075 mol/L appears to be optimal for the photooxidation in this experiment.

There are two main reasons to explain the results. Within a certain range, a higher H₂O₂ initial concentration will result in more •OH free radicals when the UV light power is fixed according to Eq. (2), and an increase in the •OH free radical concentration will promote the oxidation of Hg⁰. In other words, more •OH free radicals are available to attack atomic Hg⁰ when the H₂O₂ initial concentration increases. On the other hand, when H₂O₂ is used in excess, H₂O₂ will also act as a •OH free radical scavenger (Eq. (4) and Eq. (5)) [21,28]. Thus, the concentration of •OH free radicals decreases.



In addition, redundant •OH free radicals will dimerize to H₂O₂ (Eq. (6)) [29], also weakening the oxidation ability of the reaction system.



Consequently, the further increase in H₂O₂ initial concentration only leads to a slight contribution to the Hg⁰ removal efficiency.

3. Influence of Hg⁰ Initial Concentration

The influence of Hg⁰ initial concentration is investigated and the results are presented in Fig. 4. The increase in the Hg⁰ initial concentration from 25.3 to 83.5 μg/Nm³ causes a decrease in the Hg⁰ removal efficiency from 71.5 to 51.6%.

The influence of Hg⁰ initial concentration on Hg⁰ removal efficiency can be explained by the following reasons. First, obviously, the amount of Hg⁰ passing through the reactor per unit time increases with the increase in Hg⁰ initial concentration. As H₂O₂ initial concentration is fixed, the ratio of •OH free radicals to Hg⁰ decreases

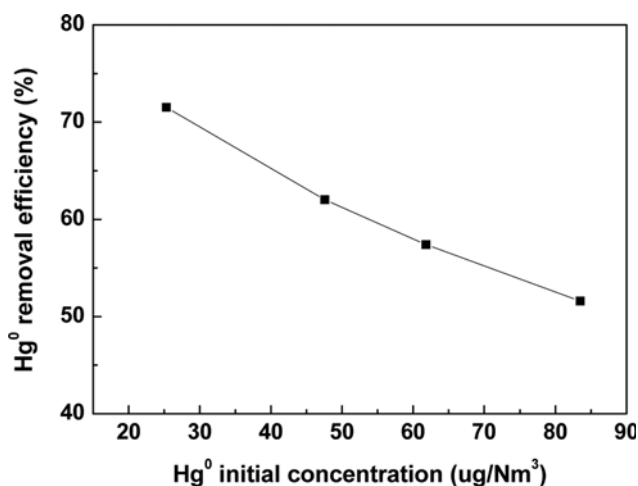


Fig. 4. Removal efficiencies of Hg⁰ under different Hg⁰ initial concentrations. Conditions: UV light power, 36 W; H₂O₂ initial concentration, 0.075 mol/L; solution initial pH, 7; O₂ percentage, 6%; H₂O₂ solution volume, 600 ml.

in the reaction system, which causes a decrease in Hg⁰ removal efficiency. Second, Hg⁰ can also absorb UV light [27]. The Lambert-Beer law equation can be used to reveal the relationship between the reincident UV light intensity and the transmitted UV light intensity [30]:

$$I = I_0 \exp(-kbc) \quad (7)$$

where I₀ is the incident light intensity, I is the transmitted light intensity, k is the light absorption coefficient, b is the thickness of light absorption layer, and c is the concentration of light absorption medium. According to Eq. (7), a rise in Hg⁰ initial concentration will lead to an exponential decay in the transmitted UV-light intensity, thus lowering the utilization efficiency of UV-light energy. Consequently, Hg⁰ removal efficiency decreases.

4. Influence of Solution Initial pH and pH Conditioning Agent

The influence of solution initial pH and pH conditioning agent on Hg⁰ removal efficiency was also investigated. This research subject aims at a potential engineering application, so we chose hydrochloric acid (HCl) and sodium hydroxide (NaOH) as the pH conditioning agents, as both are easily obtainable in the chemical industry. The solution initial pH is adjusted through the addition of either hydrochloric acid (0.5 mol/L) or sodium hydroxide (0.5 mol/L) solution with the use of an acidimeter.

The results are shown in Fig. 5. When the solution initial pH increases from 1 to 5 (solution initial pHs of 1, 3 and 5 are acquired through the addition of hydrochloric acid), the Hg⁰ removal efficiency increases. However, when the solution initial pH further increases from 5 to 11 (solution initial pHs of 7, 9 and 11 are acquired through the addition of sodium hydroxide solution), the Hg⁰ removal efficiency decreases. The highest Hg⁰ removal efficiency (56.0%) appears to be achieved at solution initial pH of 5. Meanwhile, the Hg⁰ removal efficiency in acidic media is found to be higher than that in alkaline media. From Fig. 5, we can infer that the solution

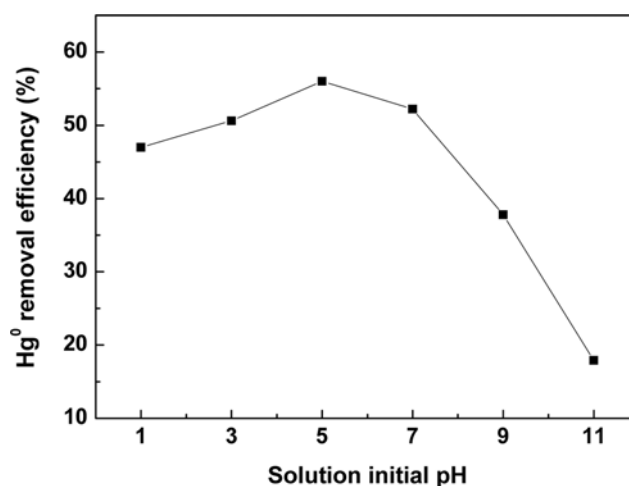


Fig. 5. Removal efficiencies of Hg⁰ under different solution initial pHs. Conditions: UV light power, 36 W; H₂O₂ initial concentration, 0.075 mol/L; Hg⁰ initial concentration, 80.9-83.9 μg/Nm³; O₂ percentage, 6%; H₂O₂ solution volume, 600 ml. Solution initial pHs of 1, 3 and 5 are acquired through the addition of hydrochloric acid, and solution initial pHs of 7, 9 and 11 are acquired through the addition of sodium hydroxide solution.

initial pH and pH conditioning agent have a remarkable synergistic effect on the Hg^0 removal efficiency.

When the pH conditioning agent is hydrochloric acid, quantities of Cl^- anions, which can compete with Hg^0 for $\bullet\text{OH}$ free radicals, are added into the solution as well. The reactions between Cl^- anion and $\bullet\text{OH}$ free radical are as follows [31]:



The intermediate and final products (ClOH^- anions, Cl atoms and Cl_2^- anions) generated from these reactions are much less reactive than $\bullet\text{OH}$ free radicals [32], so that Hg^0 removal rate is inhibited in the presence of Cl^- anions, and an increase in Cl^- anions will lead to a decrease in Hg^0 removal efficiency.

In base pH (the pH conditioning agent is sodium hydroxide), a significant decline in Hg^0 removal efficiency can be attributed to three main reasons. First, an alkaline condition will cause the instability of H_2O_2 [20,33], leading to the decomposition of H_2O_2 :



H_2O_2 molecule decomposes into water and oxygen, losing its role as the releasing agent of $\bullet\text{OH}$ free radicals. Second, an $\text{H}_2\text{O}_2/\text{HO}_2^-$ equilibrium is reached concomitant with the deprotonation of H_2O_2 on an alkaline condition:



HO_2^- anion, the conjugate base of H_2O_2 , can react with H_2O_2 according to Eq. (13) [32], which makes $\bullet\text{OH}$ free radical concentration much lower:



Third, the HO_2^- anion can also react with $\bullet\text{OH}$ free radical [34,35]:

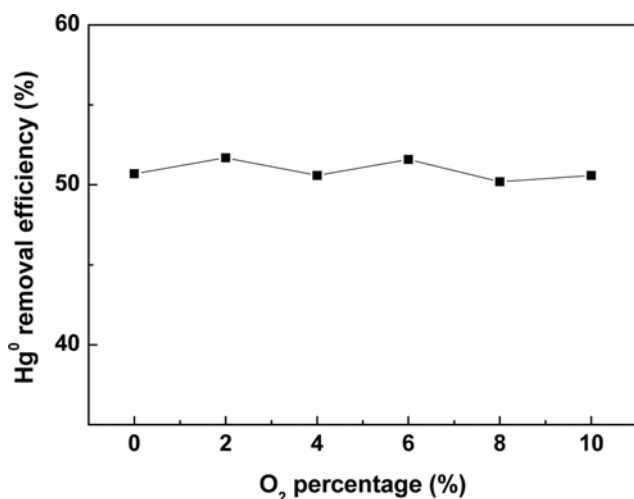


Fig. 6. Removal efficiencies of Hg^0 under different O_2 percentages. Conditions: UV light power, 36 W; H_2O_2 initial concentration, 0.075 mol/L; Hg^0 initial concentration, 82.9-85.3 $\mu\text{g}/\text{Nm}^3$; solution initial pH, 7; H_2O_2 solution volume, 600 ml.

It is reported that the reaction of HO_2^- anion with $\bullet\text{OH}$ free radical is approximately 100 times faster than its reaction with H_2O_2 molecule [32], resulting in a significant consumption of $\bullet\text{OH}$ free radical and hence inducing the great decrease in Hg^0 removal efficiency.

This paper only investigates the influence of solution initial pH and pH conditioning agent briefly, and we will do more researches to evaluate the influence comprehensively in the future, including various pH values and pH conditioning agents.

5. Influence of O_2 Percentage

The influence of O_2 percentage (volume fraction, V/V) on Hg^0 removal efficiency is shown in Fig. 6. The Hg^0 removal efficiency changes a little when the O_2 percentage ranges from 0 to 10%, meaning that the O_2 percentage has a little effect. In these experiments (see Fig. 6), the Hg^0 removal efficiency fluctuates around 51%.

The change of O_2 percentage can give rise to both positive and negative effects on Hg^0 removal efficiency. On the one hand, O_2 can react with $\bullet\text{OH}$ free radicals (Eq. (15)), reducing the probability of recombination of $\bullet\text{OH}$ free radicals to each other [30,36]:



Besides, $\bullet\text{O}$ free radical (2.05 eV) also has a strong oxidation ability and is beneficial for the oxidation of Hg^0 [27]. Therefore, the increase in O_2 percentage is conducive to the removal of Hg^0 to a certain extent. On the other hand, according to the two-film theory, a gas of high solubility will have a competitive advantage over the gas of low solubility during a gas-liquid mass transfer process [36]. As the solubility of O_2 in water is much higher than that of Hg^0 , the gas-liquid mass transfer rate of Hg^0 will be inhibited when the O_2 percentage increases, which is not beneficial for the Hg^0 removal. As a result of the combined effects of these positive and negative factors, O_2 percentage has little impact on Hg^0 removal efficiency.

6. Influence of H_2O_2 Solution Volume

Fig. 7 gives the Hg^0 removal efficiency profile under different H_2O_2 solution volumes. The experimental results show that H_2O_2 solution volume plays an important role in the Hg^0 removal efficiency. In general, an increase in the H_2O_2 solution volume will enhance

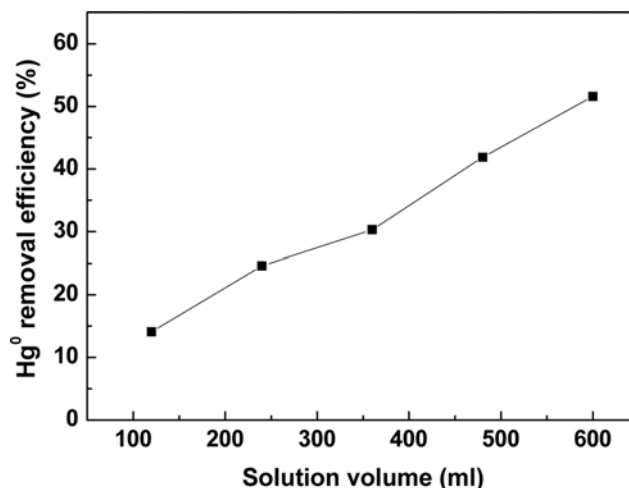


Fig. 7. Removal efficiencies of Hg^0 under different H_2O_2 solution volumes. Conditions: UV light power, 36 W; H_2O_2 initial concentration, 0.075 mol/L; Hg^0 initial concentration, 82.4-83.5 $\mu\text{g}/\text{Nm}^3$; solution initial pH, 7; O_2 percentage, 6%.

Hg⁰ removal.

The influence of H₂O₂ solution volume on Hg⁰ removal efficiency can be explained as follows. As we can see, more H₂O₂ solution volume obviously leads to a higher ratio of •OH free radicals to Hg⁰ and a longer reaction time in the reactor for Hg⁰. As a result, more Hg⁰ is removed.

CONCLUSIONS

We studied the photooxidative removal of Hg⁰ in simulated flue gas from coal-fired utilities by wet scrubbing using UV/H₂O₂ advanced oxidation process in a laboratory-scale bubble column reactor. The Hg⁰ removal efficiencies were measured at different UV light powers, H₂O₂ initial concentrations, Hg⁰ initial concentrations, solution initial pHs, O₂ percentages and H₂O₂ solution volumes. It is concluded that:

(1) Both UV light power and H₂O₂ initial concentration are critical to remove Hg⁰ in this reaction system. The Hg⁰ removal efficiency increases with the increasing of UV light power or H₂O₂ initial concentration. However, the Hg⁰ removal efficiency only has a slight increase when the H₂O₂ initial concentration goes out of a reasonable range.

(2) The influence of solution initial pHs and pH conditioning agents is investigated, and the results obtained indicate that the solution initial pH and pH conditioning agent have a remarkable synergistic effect on the Hg⁰ removal efficiency, and more research is needed to evaluate the influence comprehensively in the future.

(3) A lower Hg⁰ initial concentration or a higher H₂O₂ solution dosage will result in higher Hg⁰ removal efficiency. Meanwhile, O₂ percentage has a little effect on the Hg⁰ removal efficiency.

ACKNOWLEDGEMENT

This work is supported by the National Key Basic Research Program of China (973 Program, No. 2011CB201505) and the Transformation of Scientific and Technological Achievements Special Fund Program of Jiangsu Province (No. BA2011031).

REFERENCES

1. P. Vaithyanathan, C. J. Richardson, R. G. Kavanaugh, C. B. Craft and T. Barkay, *Environ. Sci. Technol.*, **30**(8), 2591 (1996).
2. J. H. Pavlish, E. A. Sondreal, M. D. Mann, E. S. Olson, K. C. Galbreath, D. L. Laudal and S. A. Benson, *Fuel Process. Technol.*, **82**(2-3), 89 (2003).
3. X. P. Fan, C. T. Li, G. M. Zeng, X. Zhang, S. S. Tao, P. Lu, Y. Tan and D. Q. Luo, *Energy Fuel*, **26**(4), 2082 (2012).
4. J. Munthe, H. Hultberg and A. Iverfeldt, *Water Air Soil Pollut.*, **80**(1-4), 227 (1995).
5. W. Liu, R. D. Vidic and T. D. Brown, *Environ. Sci. Technol.*, **32**(4), 531 (1998).
6. Y. Wu, S. X. Wang and D. G. Streets, *Environ. Sci. Technol.*, **40**(17), 5312 (2006).
7. X. Y. Wen, C. T. Li, X. P. Fan, H. L. Gao, W. Zhang, L. Chen, G. M. Zeng and Y. P. Zhao, *Energy Fuel*, **25**(7), 2939 (2011).
8. R. Yan, D. T. Liang, T. Tsen, Y. P. Wong and Y. L. Lee, *Fuel*, **83**(17-18), 2401 (2004).
9. F. Ding, Y. C. Zhao, L. L. Mi, H. L. Li, Y. Li and J. Y. Zhang, *Ind. Eng. Chem. Res.*, **51**(7), 3039 (2012).
10. Z. Qu, N. Q. Yan, P. Liu, J. P. Jia and S. J. Yang, *J. Hazard. Mater.*, **183**(1-3), 132 (2010).
11. E. M. Prestbo and N. S. Bloom, *Water Air Soil Poll.*, **80**(1-4), 145 (1995).
12. L. Zhang, Y. Q. Zhuo, L. Chen, X. C. Xu and C. H. Chen, *Fuel Process. Technol.*, **89**(11), 1033 (2008).
13. E. J. Granite, H. W. Pennline and R. A. Hargis, *Ind. Eng. Chem. Res.*, **39**(4), 1020 (2000).
14. A. Aleboye, M. B. Kasiri, M. E. Olya and H. Aleboye, *Dyes Pigm.*, **77**(2), 288 (2008).
15. F. H. Alhamed, M. A. Rauf and S. S. Ashraf, *Desalination*, **239**(1-3), 159 (2009).
16. Y. Lester, D. Avisar and H. Mamane, *Environ. Technol.*, **31**(2), 175 (2010).
17. A. Fujishima and K. Honda, *Nature*, **238**(5358), 37 (1972).
18. B. Chen, C. Yang and N. K. Goh, *J. Environ. Sci. - China*, **17**(6), 886 (2005).
19. N. Shigwedha, Z. Z. Hua and J. Chen, *J. Environ. Sci. - China*, **19**(3), 367 (2007).
20. Q. H. Hu, C. L. Zhang, Z. R. Wang, C. Yan, K. H. Mao, X. Q. Zhang, Y. L. Xiong and M. J. Zhu, *J. Hazard. Mater.*, **154**(1-3), 795 (2008).
21. N. Modirshahla and M. A. Behnajady, *Dyes Pigm.*, **70**(1), 54 (2006).
22. F. Yuan, C. Hu, X. X. Hu, D. B. Wei, Y. Chen and J. H. Qu, *J. Hazard. Mater.*, **185**(2-3), 1256 (2011).
23. D. Alibegic, S. Tsuneda and A. Hirata, *Chem. Eng. Sci.*, **56**(21-22), 6195 (2001).
24. C. D. Cooper, C. A. Clausen, L. Pettey, M. M. Collins and M. P. de Fernandez, *J. Environ. Eng. - Asce*, **128**(1), 68 (2002).
25. S. C. Ma, J. X. Ma, Y. Zhao and M. Su, *Proc. Chin. Soc. Electr. Eng.*, **29**(5), 27 (2009).
26. Y. X. Liu, J. Zhang, C. D. Sheng, Y. C. Zhang and L. Zhao, *Energy Fuel*, **24**(9), 4925 (2010).
27. Y. X. Liu, J. Zhang, C. D. Sheng, Y. C. Zhang and L. Zhao, *Sci. China Technol. Sci.*, **53**(7), 1839 (2010).
28. M. Muruganandham and M. Swaminathan, *Dyes Pigm.*, **62**(3), 269 (2004).
29. N. Daneshvar, M. A. Behnajady and Y. Z. Asghar, *J. Hazard. Mater.*, **139**(2), 275 (2007).
30. Y. X. Liu, J. Zhang, C. D. Sheng, Y. C. Zhang and L. Zhao, *Energy Fuel*, **24**(9), 4931 (2010).
31. G. V. Buxton, C. L. Greenstock, W. P. Helman and A. B. Ross, *J. Phys. Chem. Ref. Data*, **17**(2), 513 (1988).
32. N. Daneshvar, M. A. Behnajady, M. K. A. Mohammadi and M. S. S. Dorraji, *Desalination*, **230**(1-3), 16 (2008).
33. H. Y. Shu and M. C. Chang, *Dyes Pigm.*, **65**(1), 25 (2005).
34. E. J. Land and M. Ebert, *Trans. Faraday Soc.*, **63**, 1181 (1967).
35. M. P. Titus, V. G. Molina, M. A. Banos, J. Gimenez and S. Espluga, *Appl. Catal. B: Environ.*, **47**(4), 219 (2004).
36. M. Bobu, A. Yediler and I. Siminiceanu, *Appl. Catal. B: Environ.*, **83**(1-2), 15 (2008).